Available online at www.sciencedirect.com

ScienceDirect

*Mendeleev Commun.*, 2021, **31**, 91–93

Mendeleev Communications

# Hydrophobic mixed-metal MOF-derived carbon sponges

**Cesar M. Oliva González,[a] Ana de Monserrat Navarro Tellez,[a] Boris I. Kharisov,*[a] Oxana V. Kharissova,[a] Thelma E. Serrano Quezada[a] and Lucy T. González[b]**

[a] *Universidad Autónoma de Nuevo León, 66455 San Nicolás de los Garza, Nuevo León, México. E-mail: bkhariss@hotmail.com*

[b] *Tecnológico de Monterrey, Escuela de Ingeniería y Ciencias, 64890 Monterrey, Nuevo León, México. E-mail: lucy.gonzalez@itesm.mx*

DOI: 10.1016/j.mencom.2021.01.028

**We report the preparation of carbon sponges with highly hydrophobic and superhydrophobic metal nanoparticles from melamine–formaldehyde sponges coated with metal–organic structures based on Co, Ni and Ni–Co with rod morphology using a simple one-step carbonization method at temperatures of 300, 500 and 700 °C.**

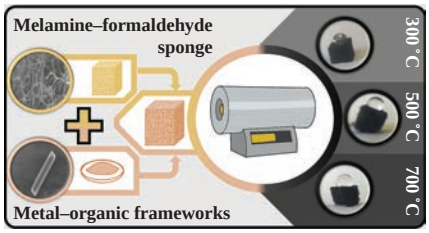


*Keywords*: carbon sponge, metal–organic frameworks, hydrophobic sponges, MOF-derived carbon, mixed-metal MOF.

Metal–organic frameworks (MOFs) have been extensively studied in the last two decades for their structural and morphological characteristics.[1,2] However, the vast majority of these materials decompose readily in the presence of moisture.[3] This fact limits their use in a wide variety of applications such as aqueous catalysis,[4] oil spill clean-up, hydrocarbon storage/separation and water treatment.[5–7] For this reason, several studies have focused on ensuring the hydrophobic properties of these materials, based mainly on two strategies: introduction of hydrophobic functional groups[8,9] and pyrolysis of MOFs.[10]

The first strategy consists of, as its name suggests, the introduction of functional groups, which are usually fluorinated or alkyl-containing compounds[11,12] with ultra-low surface energy (10–20 mN m$^{-1}$).[13,14] Although this strategy can be very efficient, only a few methods have been currently developed to synthesize hydrophobic MOFs.[15] The second strategy, based on MOF pyrolysis, is to expose these materials to high temperatures in an inert atmosphere, which removes the hydrophilic functional groups of the material. The morphological characteristics and properties of pyrolyzed MOFs can be almost entirely preserved depending on the temperature.[16,17] Also, in some cases, MOF pyrolysis can work to increase the surface area of a material[18] and even to create carbon composites with metal nanoparticles attached to their surfaces.[19,20]

In this work, we prepared hydrophobic carbon sponges by pyrolysis of melamine–formaldehyde sponges coated with bimetallic Ni–Co MOF and compared their morphological and hydrophobic characteristics with carbon sponges synthesized similarly but with monometallic (Co and Ni) MOFs. All sponges obtained in this study had contact angle values of more than 100° and metal nanoparticles on their surface, which makes them promising for use in water purification and catalysis.

The first part of this study focused on the synthesis of HKUST-type MOFs using a controlled precipitation method, starting with trimesic acid (BTC) as a ligand and cobalt(II) nitrate hexahydrate [$Co(NO_3)_2 \cdot 6H_2O$] and nickel(II) nitrate hexahydrate [$Ni(NO_3)_2 \cdot 6H_2O$] as metal center precursors. In the case of bimetallic MOF, a mixture of salts with a molar ratio of 1 : 1 was used.

The diameter of rod-shaped particles was found to be in the range of 350–385, 387–454 and 436–487 nm for the BTC-Ni, BTC-Co and BTC-(Ni–Co) MOFs, respectively (Figure 1).† As one can see from these measurements, the particle size is similar for monometallic MOFs and slightly larger for bimetallic MOFs. The results of element mapping show a homogeneous dispersion in each case. It is noteworthy that MOF BTC-(Ni–Co) displays signals of both metals [see Figure 1(*d*)–(*f*)] used for its synthesis. This fact indicates that both cobalt and nickel have been successfully integrated and are not just a mixture of individual MOFs. It is important to note that in all cases, MOFs have the shape of a rectangular bar. It is probably because large hedgehog-shaped structures were originally formed, which were fragmented by ultrasound treatment during synthesis.

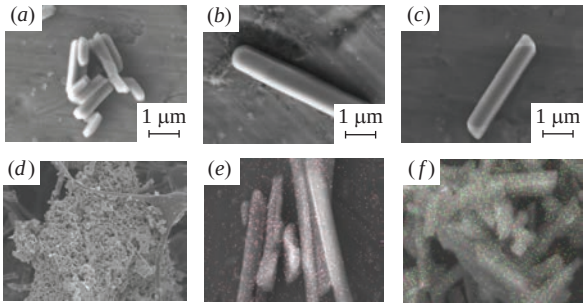


**Figure 1** SEM micrographs of (*a*) BTC-Ni, (*b*) BTC-Co and (*c*) BTC-(Ni–Co) MOFs and elemental mapping performed with the EDX technique for (*d*) BTC-Ni, (*e*) BTC-Co and (*f*) BTC-(Ni–Co) MOFs. The areas highlighted in green and pink represent nickel and cobalt signals, respectively.

† A scanning electron microscope (SEM) JEOL JSM6701F was used for the morphological characterization of melamine–formaldehyde, MOFs and carbon sponges.

The second part of this study focused on the formation of hydrophobic carbon sponges. Initially, the addition of MOFs to sponges, which are commercially available and produced by BASF company, was accomplished by a simple immersion method, dipping melamine–formaldehyde sponges into an ethanol dispersion of the corresponding MOF. Subsequently, the sponges were dried. Finally, the sponges, loaded with MOF, were subjected to pyrolysis in a quartz tube inside the tubular furnace at the temperature of 300, 500 or 700 °C for 1 h in the flow of nitrogen of chromatographic quality.

In general, the BTC MOFs on melamine sponge heated at the temperature of 300 °C did not demonstrate noticeable changes in their morphology, retaining the shape of the bar and surface without visible roughness. When samples were exposed to the temperature of 500 °C, the particles of spherical morphology began to appear on their surface. In the case of BTC-Ni, these particles are less visible and range in size from 46.3 to 77.9 nm. In contrast, the BTC-Co and BTC-(Ni–Co) MOFs on the melamine sponge begin to lose their initial morphology in addition to increasing their roughness and the appearance of particles with sizes in the range of 82–183 and 241.5–325.4 nm, respectively.

Observing the micrographs of BTC MOFs on melamine sponge pyrolyzed at 700 °C, one can see that BTC-Ni MOF continues to retain its initial morphology, but the spherical particles are more pronounced compared to those observed after pyrolysis at 500 °C and their size is in the range from 41.4 to 64.8 nm. The BTC-Co and BTC-(Ni–Co) MOFs are still very similar to each other when exposed to a temperature of 700 °C. In both cases, the small particles that we observe at a temperature of 500 °C agglomerate to form larger and irregular particles. The agglomerates of particles formed after the pyrolysis of the BTC-Co and BTC-(Ni–Co) MOFs at 700 °C have sizes ranging from 172.5 and 96.0 nm to 242.9 and 267.5 nm, respectively.

Figure 2† shows the evolution of morphology demonstrated by the sponge coated with the bimetallic MOF when subjected to pyrolysis at the temperature of 300, 500 or 700 °C. The insets show how the resulting sponges interacted with a drop of water, leading to the conclusion that the untreated material had hydrophilic properties, while all the other sponges subjected to pyrolysis had a hydrophobic character. A drop of water could be present on their surface without entering their pores. It should be mentioned that placing the drop of water on the carbon sponge obtained from BTC-(Ni–Co) at 700 °C was a difficult task since the drop moved very easily on the surface of the sponge, which gave us indications on the superhydrophobic nature of this material.

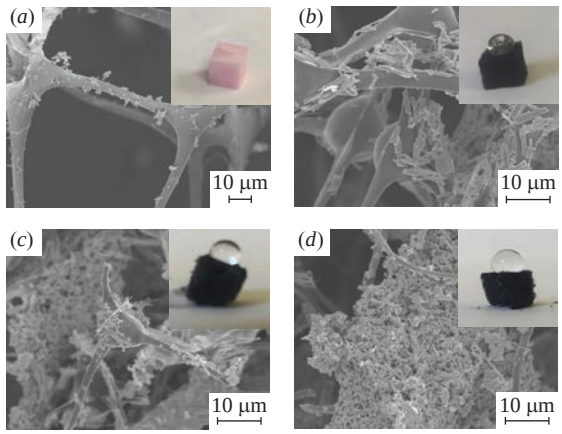


**Figure 2** SEM micrographs and photographs (in the inset) of the sponge coated with BTC-(Ni–Co) (*a*) before pyrolysis and after pyrolysis at (*b*) 300, (*c*) 500 and (*d*) 700 °C under a nitrogen atmosphere.

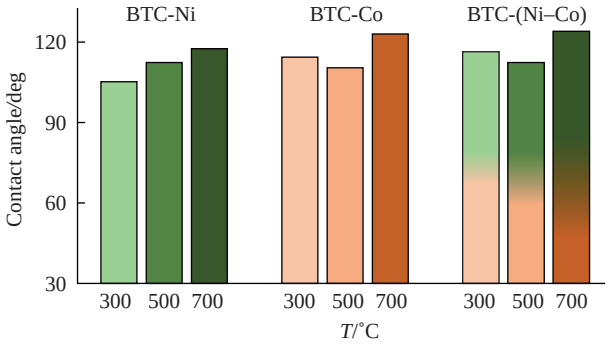


**Figure 3** Contact angle of water on the surface of carbon sponges prepared from the melamine–formaldehyde sponges coated with BTC-Ni, BTC-Co or BTC-(Ni–Co) MOFs by pyrolysis at 300, 500 or 700 °C under nitrogen atmosphere.

To quantitatively compare the hydrophobicity of the obtained carbon sponges, we measured their contact angle (°) between water and the surface of the sponges. A summary of these results is shown in Figure 3.‡ Solid smooth surfaces can be considered as hydrophilic ($\theta = 0°$), weakly hydrophilic ($0° < \theta < 65°$), weakly hydrophobic ($65° < \theta < 90°$) and hydrophobic ($90° < \theta < 120°$) according to the classification of hydrophobic surfaces proposed by J. Drelich *et. al.*[21] It is evident that all the pyrolyzed sponges possess hydrophobic properties by far exceeding the contact angle of 90°, which is the minimum required for their application in the successful separation, absorption and removal of nonpolar compounds dispersed in water.

Sponges exposed to the temperature of 300 °C are hydrophobic, which can be explained by the loss of uncoordinated electronegative groups that were eliminated as water during pyrolysis, reducing the wettability of the material. On the contrary, an increase in the contact angle of carbon sponges prepared at 700 °C is attributed to a combination of two factors: the first is the absence of hydrophilic groups, and the second is an increase in the roughness on the fiber surface caused by the appearance of spherical nanoparticles. These nanoparticles reduce the adhesion of water droplets by forming small air cushions in the cavities between them.

Besides, there is a tendency that the higher the pyrolysis temperature, the larger the contact angle of the carbon sponge. This is true only for sponges obtained by pyrolysis of the sponges coated with BTC-Ni and can be explained by the fact that the bar morphology is preserved at all pyrolysis temperatures, as observed in the micrographs of the material. In contrast, the sponges made from BTC-Co and BTC-(Ni–Co) MOFs expand and lose their morphology when exposed to the treatment at 500 °C. Furthermore, at this temperature, sufficient cavities have not yet appeared to form the air cushions mentioned above, and this causes a slight loss of surface roughness, which leads to a decrease in the contact angle.

In conclusion, hydrophobic carbon sponges were obtained successfully by pyrolysis of melamine–formaldehyde sponges coated with MOF. All the sponges presented contact angles greater than 100°. The physical characteristics of these materials may limit their applications. The sponges obtained at 700 °C are very fragile to be subjected to processes in which they can break down, such as adding them in strong stirring reactions. On the contrary, the materials produced at 300 and 500 °C can be compressed and readily recovered in their morphology, so these carbon sponges can be adapted for the desired application.

‡ Contact angle was determined by means of the ImageJ software, using the DropSnake plugin and the LB-ADSA (low bond axisymmetric drop shape analysis) plugin.

A preliminary evaluation of the observed properties indicates that these materials can potentially be useful in the separation of non-polar contaminants dispersed in water.

This work was supported by the CONACyT (Ph. D. scholarship for Cesar M. Oliva González) and the Department of Chemistry of the Universidad Autónoma de Nuevo León (Monterrey, Mexico).

## References

1 L. Jiao, Y. Wang, H.-L. Jiang and Q. Xu, *Adv. Mater.*, 2018, **30**, 1703663.
2 L. M. Kustov, V. I. Isaeva, J. Přech and K. K. Bisht, *Mendeleev Commun.*, 2019, **29**, 361.
3 Y.-J. Lee, Y.-J. Chang, D.-J. Lee and J.-P. Hsu, *J. Taiwan Inst. Chem. Eng.*, 2018, **93**, 176.
4 K. Yuan, T. Song, D. Wang, X. Zhang, X. Gao, Y. Zou, H. Dong, Z. Tang and W. Hu, *Angew. Chem.*, 2018, **130**, 5810.
5 N. Zhao, P. Li, X. Mu, C. Liu, F. Sun and G. Zhu, *Faraday Discuss.*, 2017, **201**, 63.
6 S. Yuan, L. Feng, K. Wang, J. Pang, M. Bosch, C. Lollar, Y. Sun, J. Qin, X. Yang, P. Zhang, Q. Wang, L. Zou, Y. Zhang, L. Zhang, Y. Fang, J. Li and H.-C. Zhou, *Adv. Mater.*, 2018, **30**, 1704303.
7 V. V. Arslanov, M. A. Kalinina, E. V. Ermakova, O. A. Raitman, Yu. G. Gorbunova, O. E. Aksyutin, A. G. Ishkov, V. A. Grachev and A. Yu. Tsivadze, *Russ. Chem. Rev.*, 2019, **88**, 775.
8 M.-L. Gao, S.-Y. Zhao, Z.-Y. Chen, L. Liu and Z.-B. Han, *Inorg. Chem.*, 2019, **58**, 2261.
9 S. Roy, V. M. Suresh and T. K. Maji, *Chem. Sci.*, 2016, **7**, 2251.
10 X. Sun, T. Wu, Z. Yan, W.-J. Chen, X.-B. Lian, Q. Xia, S. Chen and Q.-H. Wu, *J. Solid State Chem.*, 2019, **271**, 354.
11 M. Joharian, A. Morsali, A. A. Tehrani, L. Carlucci and D. M. Proserpio, *Green Chem.*, 2018, **20**, 5336.
12 M. Ding, X. Cai and H.-L. Jiang, *Chem. Sci.*, 2019, **10**, 10209.
13 Z. Zhang and X.-Y. Liu, *Chem. Soc. Rev.*, 2018, **47**, 7116.
14 D. Ahmad, I. van den Boogaert, J. Miller, R. Presswell and H. Jouhara, *Energy Sources, Part A*, 2018, **40**, 2686.
15 K. Jayaramulu, F. Geyer, A. Schneemann, Š. Kment, M. Otyepka, R. Zboril, D. Vollmer and R. A. Fischer, *Adv. Mater.*, 2019, **31**, 1900820.
16 Y.-F. Zhang, L.-G. Qiu, Y.-P. Yuan, Y.-J. Zhu, X. Jiang and J.-D. Xiao, *Appl. Catal., B*, 2014, **144**, 863.
17 J.-K. Sun and Q. Xu, *Energy Environ. Sci.*, 2014, **7**, 2071.
18 S. J. Yang, T. Kim, J. H. Im, Y. S. Kim, K. Lee, H. Jung and C. R. Park, *Chem. Mater.*, 2012, **24**, 464.
19 J. Gu, H. Fan, C. Li, J. Caro and H. Meng, *Angew. Chem., Int. Ed.*, 2019, **58**, 5297.
20 L. M. Tijerina, C. M. Oliva González, B. I. Kharisov, T. E. Serrano Quezada, Y. Peña Méndez, O. V. Kharissova and I. Gómez de la Fuente, *Mendeleev Commun.*, 2019, **29**, 400.
21 J. Drelich, E. Chibowski, D. D. Meng and K. Terpilowski, *Soft Matter*, 2011, **7**, 9804.

*Received: 16th October 2020; Com. 20/6340*